

A new Fe-based metallic glass with a larger supercooled liquid region

K. Q. QIU*, Y. L. REN

School of Material Sciences and Engineering, Shenyang University of Technology, 58 South Xinghua Street, Shenyang 110023, People's Republic of China
E-mail: kqniu@yahoo.com.cn

Fe-based amorphous alloys are widely studied because of their lower raw material cost in preparation and higher mechanical or magnetic properties [1, 2] in application. Search of new Fe-based alloys with a better glass-forming ability and a larger supercooled liquid region (ΔT_x , defined by the temperature interval between crystallization temperatures T_x and glass-transition temperatures T_g) is of great interest because it can widen application and improve thermal stability against crystallization [3–5]. The larger supercooled liquid region implies that a longer duration time and a wider temperature range are expected during warm-working of amorphous alloys into various bulk shapes through the viscous flowability of the supercooled liquid.

For ternary Fe-based alloys, a large ΔT_x that was found by an addition of transition metals such as niobium and zirconium respectively, to the Fe–B based system can reach as high as 71 K for Fe–Nb–B [6] and 83.2 K for Fe–Zr–B [7] alloy systems. The atomic radii of beryllium and boron are the smallest, except carbon, among possible metallic and metalloid alloying elements respectively. Both of them are lower than that of iron element. Compared with previous Fe-based bulk metallic glasses, Fe–B–Be alloy has a different atomic size distribution which is expected to have higher GFA according to Senkov's analyses [8]. Therefore, a new alloy composition, i.e., $\text{Fe}_{80-x}\text{B}_{20}\text{Be}_x$ ($x = 20, 25, 30, 35$) alloys, was designed and examined in this paper.

The ternary alloys with composition of $\text{Fe}_{80-x}\text{B}_{20}\text{Be}_x$ ($x = 20, 25, 30, 35$, in atomic percentage) were prepared by arc melting the mixture of pure Fe, Be metals and commercial Fe–B alloy, which contains 80.2 wt.% of Fe, 17.6 wt.% of B and 2.2 wt.% of other constituents, such as Si, C, P and S etc, under a Ti-gettered argon atmosphere. The purity of pure metals is about 99.5% in weight percent. Rapidly solidified ribbons with thickness of 40, 65 μm and a width of 5 mm were prepared by a single roller melt spinning the master ingots in an argon atmosphere. The amorphous structure was examined by X-ray diffractometer (XRD) using $\text{CuK}\alpha$ radiation. Thermal stability associated with glass-transition temperature, supercooled liquid region and crystallization temperature was examined by differential scanning calorimeter (DSC) at a heating rate of 20 K/min. The onset and offset melting temperatures of the alloys were determined by using differential thermal analysis (DTA).

Fig. 1 shows the XRD patterns for the $\text{Fe}_{80-x}\text{B}_{20}\text{Be}_x$ ($x = 20, 25, 30$ and 35, respectively) ribbons with thickness of 40 μm . It is obvious that the alloys with $x = 20$ and 25 are almost in amorphous state and a broad diffraction maximum in the range of $35 < 2\theta < 55^\circ$ are present. In others some crystalline diffraction peaks are superimposed on the amorphous halo. With further increasing the ribbon's thickness to 65 μm , the as-cast $\text{Fe}_{50}\text{B}_{20}\text{Be}_{30}$ alloy contains more amorphous phase than $\text{Fe}_{52}\text{B}_{20}\text{Be}_{25}$ alloy as shown in Fig. 2. Therefore the $\text{Fe}_{50}\text{B}_{20}\text{Be}_{30}$ exhibits the largest GFA among the alloys concerned.

DSC scans for the amorphous alloys with a thickness of 40 μm are shown in Fig. 3. For each of the two alloys, an endothermic event due to the glass-transition is observed, followed by an exothermic peak as the metastable supercooled liquid transforms into equilibrium crystalline phases. The glass-transition temperature, T_g , and the crystallization temperature, T_x , defined by the onset temperatures of the endothermic and exothermic events, respectively, are 787 and 837 K for the $\text{Fe}_{55}\text{B}_{20}\text{Be}_{25}$ amorphous alloy, 812 and 867 K for $\text{Fe}_{50}\text{B}_{20}\text{Be}_{30}$ amorphous alloy, respectively. The supercooled liquid regions are 50 K for the former and 55 K for the latter. The very large supercooled liquid region before crystallization for $\text{Fe}_{50}\text{B}_{20}\text{Be}_{30}$ amorphous alloy indicates that it has a high thermal stability and workability during warm-working process. No glass-transition for binary $\text{Fe}_{80}\text{B}_{20}$ amorphous alloy was observed on the DSC curve at heating rate of 40 K/min and crystallization event occurred at $T_x = 745.7$ K [7]. The existence of glass-transition and supercooled liquid region means that the ternary alloys are metallic glass. The larger supercooled liquid region is corresponding to the larger GFA as many investigators observed [9–11]. In order to investigate the reason of better GFA for $\text{Fe}_{50}\text{B}_{20}\text{Be}_{30}$ alloy we have checked the melting behaviors of $\text{Fe}_{80-x}\text{B}_{20}\text{Be}_x$ alloys as shown in Fig. 4. Each of them has at least two melting peaks, indicating that they are all off eutectic composition. The changes of onset melting temperature, T_m , the offset melting temperature, T_1 , and the temperature interval between them, ΔT_m , are given in Fig. 5. It can be seen that the correlation between T_m and composition is weak which indicates that there is a eutectic melting plane near T_m . The offset melting temperatures, however, varies with the composition of the alloys. Therefore the temperature interval ΔT_m changes too. For $\text{Fe}_{50}\text{B}_{20}\text{Be}_{30}$ alloy,

*Author to whom all correspondence should be addressed.

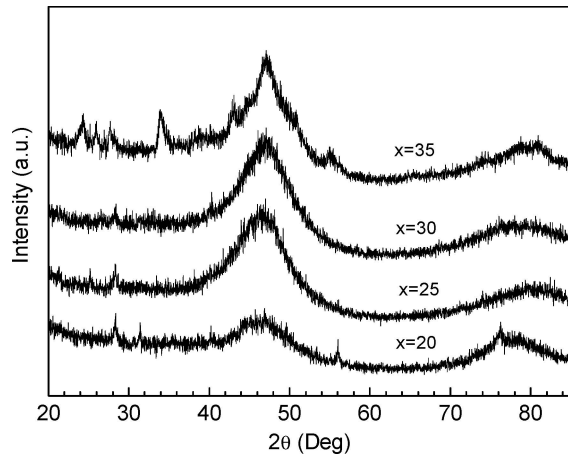


Figure 1 XRD patterns taken from $\text{Fe}_{80-x}\text{B}_{20}\text{Be}_x$ ($x = 20, 25, 30$ and 35 respectively, marked in the figure) ribbons with a thickness of $40 \mu\text{m}$.

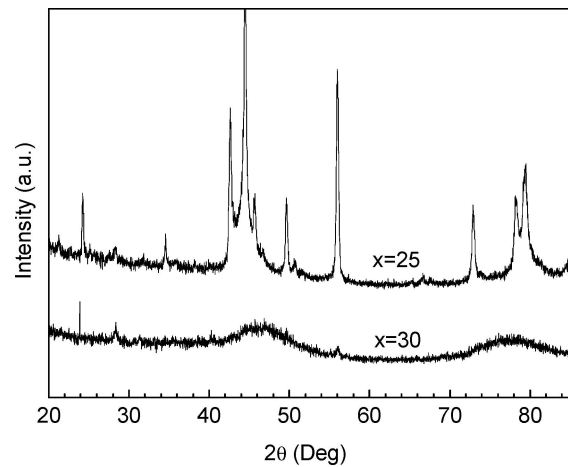


Figure 2 XRD patterns taken from $\text{Fe}_{80-x}\text{B}_{20}\text{Be}_x$ ($x = 25$ and 30 as marked in the figure) ribbons with a thickness of $65 \mu\text{m}$.

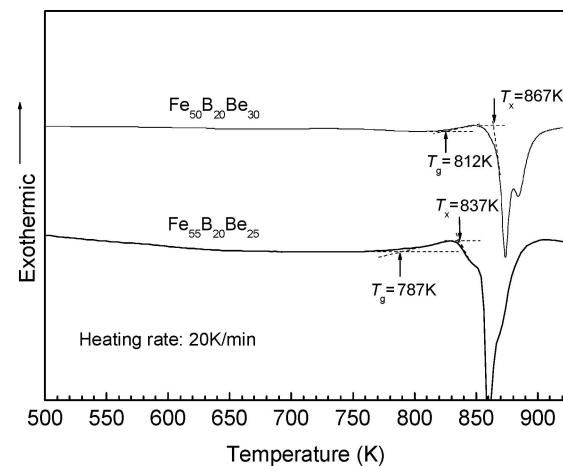


Figure 3 DSC traces obtained at heating rate of 20 K/min for $\text{Fe}_{55}\text{B}_{20}\text{Be}_{25}$ and $\text{Fe}_{50}\text{B}_{20}\text{Be}_{30}$ amorphous alloys.

it has the lowest T_1 and is corresponding to the lowest ΔT_m , which may be the reason why it exhibits the largest GFA [12].

The atomic sizes and relative numbers of atoms are the two most important topological parameters in destabilization of the crystal lattice [7]. The atomic radii of alloying and host elements are 0.1128 nm for beryllium, 0.082 nm for boron and 0.12412 nm for iron. The

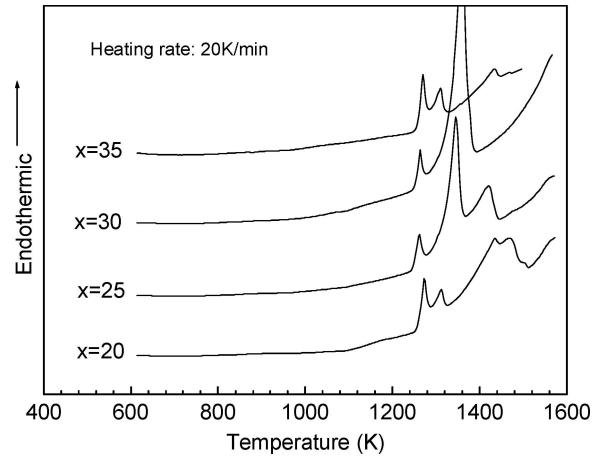


Figure 4 DTA traces obtained at heating rate of 20 K/min for $\text{Fe}_{80-x}\text{B}_{20}\text{Be}_x$ ($x = 20, 25, 30$ and 35 respectively, marked in the figure).

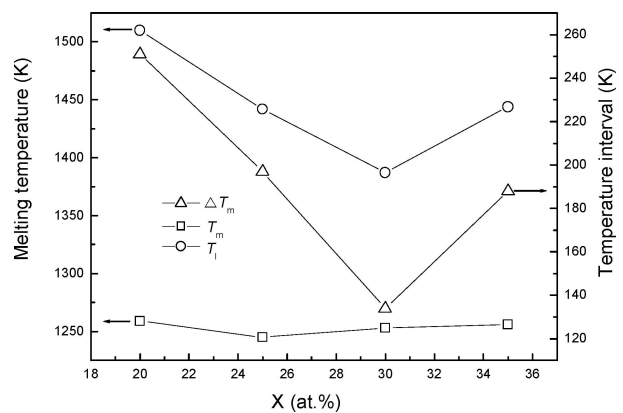


Figure 5 T_m , T_1 and ΔT_m as a function of Be content in the $\text{Fe}_{80-x}\text{B}_{20}\text{Be}_x$ ($x = 20-35$) alloys.

radii of both of the alloying elements are smaller than that of the base element. Therefore alloying elements can occupy both interstitial and substitutional sites and produce attractive short-range order complexes, and a higher fraction of the elements in the interstitial sites is required to destabilize the crystal lattice [7]. This causes a higher packing density. The higher the packing density, the higher is the thermal stability [3]. The increased concentration of interstitials should produce a dramatic softening of shear modulus and a decrease in melting temperature [13]; and at a critical concentration the melting transformation changes from first order to second order. Such a defective crystal becomes absolutely unstable and undergoes a continuous transformation to the supercooled liquid (frozen glassy state).

It should be pointed that atomic size mismatch may not be the only one reason that destabilizes the crystal lattice. Many other reasons, such as the interaction between atoms, the configuration of entropy and chemical band effect, etc. may also play an important role in amorphization of glass-forming alloys. The role of each of them may be different in different glass-formation system. Therefore many attempts, such as three empirical rules [14], reduced glass-transition temperature T_{rg} (T_g/T_1) [15], supercooled liquid region [16] have been made to explain GFA of glass-forming alloys. Among them, the reduced glass-transition

temperature T_{rg} is one of the widely used indicators of GFA of alloys due to the glass-formation composition range generally coinciding with a eutectic region. T_{rg} for the $\text{Fe}_{55}\text{B}_{20}\text{Be}_{25}$ and $\text{Fe}_{50}\text{B}_{20}\text{Be}_{30}$ are 0.528 and 0.585, respectively. Therefore $\text{Fe}_{50}\text{B}_{20}\text{Be}_{30}$ exhibited a relatively large GFA.

In the present $\text{Fe}_{80-x}\text{B}_{20}\text{Be}_x$ ($x = 20-35$) alloys, a larger supercooled liquid region as high as 55 K, which is corresponding to its higher GFA, was found in $\text{Fe}_{50}\text{B}_{20}\text{Be}_{30}$ alloy. Atomic difference in $\text{Fe} > \text{Be} > \text{B}$ series may soften shear modulus and decrease melting temperature that coincides with the larger supercooled liquid region, which increases the GFA of $\text{Fe}_{50}\text{B}_{20}\text{Be}_{30}$ alloy.

Acknowledgments

The work was supported by the Nature Sciences Foundation of Liaoning Province. Grant No. 20031036.

References

1. K. AMIYA, A. URATA, N. NISHIYAMA and A. INOUE, *Mater. Trans.* **45** (2004) 1214.
2. C. H. SMITH, "Rapidly Solidified Alloys," edited by H. H. Lieberman (Marcel Dekker, New York, 1993) p. 617.

3. T. ZHANG, A. INOUE and T. MASUMOTO, *Mater. Trans. JIM* **32** (1991) 1005.
4. A. INOUE, T. ZHANG and T. MASUMOTO, *J. Non-Cryst. Solids* **473** (1993) 156.
5. A. INOUE, H. KOSHIBA, T. ZHANG and A. MAKINO, *J. Appl. Phys.* **83** (1998) 1967.
6. T. ITOI and A. INOUE, *Mater. Trans. JIM* **40** (1999) 643.
7. L. MA and A. INOUE, *Mater. Lett.* **38** (1999) 58.
8. O. N. SENKOV and D. B. MIRACLE, *Mater. Res. Bull.* **36** (2001) 2183.
9. A. INOUE, Y. SHINOHARA and J. S. GOOK, *Mater. Trans. JIM* **36** (1995) 1427.
10. A. INOUE and A. KATSUYA, *Mater. Trans. JIM* **37** (1996) 1332.
11. E. MATSUBARA, S. SATO, M. IMAFUKU, T. NAKAMURA, H. KOSHIBA, A. INOUE and Y. WASEDA, *Mater. Trans. JIM* **41** (2000) 1379.
12. K. Q. QIU, H. F. ZHANG, A. M. WANG, B. Z. DING and Z. Q. HU, *Acta Mater.* **50** (2002) 3567.
13. A. V. GRANTO, *Phys. Rev. Lett.* **68** (1992) 974.
14. A. INOUE, *Acta Mater.* **48** (2000) 279.
15. Y. LI, S. C. NG, C. K. ONG, H. H. HNG and T. T. GOH, *Scr. Mater.* **36** (1997) 783.
16. A. INOUE, "Bulk Amorphous Alloys Preparation and Fundamental Characteristics" (Trans Tech Publications, Brindrain, Switzerland, 1998) p. 37.

*Received 2 October
and accepted 2 November 2004*